

# Using Global Simulations of the Magnetosphere for Multi-Satellite Mission Planning and Data Analysis

Joachim Raeder

Institute of Geophysics and Planetary Physics, University of California, Los Angeles

Vassilis Angelopoulos

Space Sciences Laboratory, University of California, Berkeley

**Abstract.** We use global simulations of Earth's magnetosphere to assess the scientific return from a multi-satellite mission in the magnetosphere. We examine 4 different scenarios with 20, 40, 80, and 160 satellites, respectively. The satellite orbits are randomized with perigee distances ranging from 2 to  $5R_E$ , apogee distances between 10 and  $50R_E$ , and within  $\pm 5R_E$  of the geocentric solar ecliptic (GSE) equator. For each of these satellite configurations we examine the expected observations during a typical substorm by using time traces obtained from a global simulation at the satellite positions. The 160 satellite configuration yields sufficient information to distinguish between different substorm models without any temporal/spatial ambiguities. An 80 satellite configuration still provides sufficient information for this task, however for fewer events with good satellite conjunctions and with less statistical certainty. For constellations with fewer than 40 satellites time - space ambiguities are likely to remain in the observation. However, any multi-satellite constellation would be a quantum leap in magnetospheric research because of the unprecedented coverage of other regions, because it would enable new measurement techniques that are unique to multi-satellite missions, and because it would enable the use of data assimilation techniques in global models for the first time.

## 1. Introduction

During the past 30 years the study of Earth's magnetosphere and its interaction with the solar wind has been based mainly on observations made by one or a few satellites at a time. Despite this limitation, these missions have provided a wealth of information and allowed to map out Earth's space environment for the first time and in great detail. However, these missions have also taught us that the interaction between the magnetosphere and the solar wind is a very dynamic one, and that substantial spatio-temporal ambiguities remain without multi-satellite coverage. In many cases this has precluded a thorough understanding of the solar wind-magnetosphere coupling processes, one of the more prominent examples being the physical process that leads to auroral substorms. The use of only one or a few satellites has been shown to be insufficient for the development of an unambiguous phenomenological model. For studying single substorm events few observation points do not permit a unique determination of the propagation direction of disturbances. Similarly, statistical studies are plagued by sparse data bases that leave too much room for ambiguities in the interpretation. As a consequence, the starting location of a substorm, let alone the underlying physical process of substorm initialization in the tail, is still very much in debate. Similar arguments can be made for other critical magnetospheric processes such as magnetopause reconnection, or plasma entry into the magnetosphere.

The current ISTP mission goes a step further, and provides at times about a dozen spacecraft to study the interaction. However, because

of the orbital dynamics, good conjunctions between the satellites are few, fortuitous and thus unoptimized. While ISTP, with its coordinated measurements, has helped to answer many questions, it is still not able to study the above mentioned regions with sufficient sampling.

Recent technological advances make it now possible to build satellites that are one to two orders of magnitude smaller than the typical satellites of the ISTP era. Thus, missions with tens, and maybe hundreds of satellites have become a real possibility. Such size reduction also requires simpler payloads, which at a minimum would be a magnetometer and a small ion spectrometer. Also, the data rates per satellite would be relatively small, on the order of one vector magnetic field measurement per second, and a set of ion moments every 5-10 seconds. At a first glance, this seems to be a step back from our current capabilities. However, for many of the fundamental problems mentioned above, no more than these parameters (essentially the MHD parameters) are required. For example, the study of substorm initialization requires the tracking of fronts, such as the depolarization front and the spatial boundaries of bursty bulk flows (BBFs). Similarly, studying the dayside reconnection topology requires magnetic field and plasma flow measurements in the first place, concurrent with monitoring the magnetic field conditions in the adjacent magnetosheath. In fact, for many studies magnetometers alone may be sufficient, if employed in large enough numbers.

Because of the differences in instrumentation, multi-satellite missions (MSMs) should be viewed as complementary to the fully instrumented, ISTP - like missions. Many plasma physical processes, like composition dynamics or plasma waves, cannot be addressed by a MSM. However, the MSM would remove the ambiguities that are so painfully inherent to the data obtained by the current missions. The same can be said for the upcoming magnetospheric imaging missions, like IMAGE. While certainly an improvement, remote imaging has inherent limitations as to the spatial and temporal resolution, as well as to the spatial coverage. Like with the ISTP class missions, MSM would excellently complement imaging missions.

In spite of the intuitively obvious benefits of a MSM, several questions remain to be answered quantitatively for the community to assess its feasibility and value. In particular, one needs to determine how many satellites are needed, how they should be placed into orbit, and how the data should be analyzed in order to yield maximum information of the state of the magnetosphere, its dynamics, and the physical processes. It is rather difficult to conceptualize the scientific return of such a mission particularly since we possess vernacular, explanatory models, and analysis tools borne from single satellite investigations. We therefore use in this paper global simulations of Earth's magnetosphere and ionosphere to address some of the questions involved. We first calculate orbits for several different MSM scenarios. We then let the satellites fly through the model for a brief time period and sample the modeled parameters. Because the simulation model is based on

the MHD approximation, the simulated satellite response is very similar to what is expected from a real MSM. We then use the simulated time traces to evaluate if the virtual satellites can ‘see’ what the global simulation predicts. For this purpose it is not critical that the global simulation is correct in every detail, but it is mainly important that the simulation predicts the gross features of the magnetosphere and its dynamics. Previous studies [Raeder, 1995; Raeder et al., 1997; Frank et al. 1995; Berchem et al., 1998] have shown that current, state-of-the-art global models are quite capable of predicting the state of the magnetosphere and its dynamics to the required accuracy.

In the following, we briefly introduce the model and the orbital parameters used for this study. We then analyze the results from one set of orbital parameters in more detail, and finally summarize our results and discuss the implications.

## 2. The Model

For this study we use a global MHD code which is coupled with an ionospheric model for the closure of field-aligned currents. The model features a large simulation volume, reaching several hundred  $R_E$  in the anti-sunward direction and about  $50 R_E$  in the directions transverse to the sun-Earth line. Although the model basically solves the ideal MHD equations for the magnetosphere, numerical effects, such as diffusion, viscosity, and resistivity, are necessarily introduced by the numerical methods. These permit viscous interactions and to a limited extent magnetic field reconnection. The only explicit diffusive term is the anomalous resistivity that is included in Ohm’s law. This term was in previous studies [Raeder, 1995; Raeder et al., 1996] found to be necessary to produce the correct substorm dynamics.

The MHD equations are only solved in the volume outside of  $3.5 R_E$  geocentric distance from Earth. Closer to Earth a static dipole field is assumed which connects the magnetosphere with the ionosphere. Field aligned currents that are generated in the magnetosphere are mapped along the dipole field from  $3.5 R_E$  into the ionosphere. The two-dimensional ionosphere submodel takes the mapped field-aligned currents as input and computes the ionospheric potential pattern. The potential is then mapped back to the  $3.5 R_E$  boundary and used as boundary condition for the MHD electric and velocity field.

A current limitation of the model is the lack of a ring current and plasmasphere, which makes results within about  $5 R_E$  meaningless. However, for this study the inner magnetosphere is of no importance. A more thorough discussion of the model can be found elsewhere [Raeder, 1995; Raeder et al., 1996, 1997, 1998]

## 3. Satellite Orbits

The scientific return of a MSM critically depends on the choice of the satellite orbits. The orbit selection is constrained by several factors, mainly by the way in which the satellites are launched, whether or not the satellites provide their own propulsion, whether or not the satellite orbits should be ordered and controlled, and by the selection of magnetospheric regions that are targeted for investigation.

For this paper the assumed objective is the study of the tail and substorms. Thus we wish to place the satellites into orbits near to the ecliptic plane and spread the apogee distances between about  $10 R_E$  and  $50 R_E$ . We assume that the satellites are released from a mothership with its perigee at  $2 R_E$  geocentric distance. In order to spread the apogee distances, the satellites are grouped into 4 clusters which are released at perigee with different velocities in order to attain the desired apogee distances. For a given apogee distance  $R_A$  and perigee distance  $R_p$  this velocity can be easily calculated by using the formula

$$V = (7.9 \text{ km/s}) \times \sqrt{(2/R_A) - 2/(R_A + R_p)} \quad [\text{Boden, 1991}].$$

The apogees were chosen to be 14, 20, 30, and  $45 R_E$ , respectively. The release of the satellites commences at fall equinox (September 21) from the position  $(0, 2, 0) R_E$  in Geocentric Solar Ecliptic (GSE) coordinates. The satellite orbits were then further randomized by giving each satellite a 200 m/s ‘kick’ in random directions at the first perigee pass after release. The process of randomization essentially simulates the effect of lunar, solar and J2 perturbations in the orbits that are unavoidable in the absence of probably unaffordable station keeping. With these parameters, the orbits quickly randomize and spread the satellites over a substantial area of the GSE equatorial plane.

Figure 1 shows snapshots of the satellite orbits approximately 9 months after launch for four scenarios with 20, 40, 80, and 160 satellites, respectively. After this time the orbits have precessed such that their apogees now lie close to the tail center. Except for the number of satellites all parameters are kept the same for each of the scenarios. The dots show the instantaneous position, while the lines show one hour of the orbit. The perigee distances range from about 2 to  $5 R_E$  and the apogee distances range from about 10 to  $50 R_E$ , with orbital periods of 0.8 to 7.5 days. The orbits extend to about  $\pm 15 R_E$  in the Y direction and about  $\pm 5 R_E$  in the Z direction, and thus cover the most interesting regions for substorm studies. Of course, during the course of a year the orbits sweep through all local times and provide opportunity for numerous other studies, such as the boundary layers, the magnetopause, the magnetosheath, and the bow shock. For this study, however, we concentrate on the tail and substorms.

Because the satellites move very slowly near apogee, they are virtually stationary in the tail compared to typical substorm time scales. The orbital dynamics also assures that the satellites spend most of their time in the tail, thus for a large number of satellites at least 80% of the satellites are in the tail at any given time.

Figure 2 shows a rendering of the magnetosphere just after a substorm onset. The colored planes (at  $X_{GSE} = -40 R_E$  and  $Y_{GSE} = 0 R_E$ ) show color coded the plasma pressure, clearly depicting the bow shock, the magnetopause, the tail lobes, and the plasma sheet. The sphere at the coordinate center shows the inner boundary of the simulation at  $3.5 R_E$ . The set of light blue field lines originates from  $66^\circ$  magnetic latitude and indicates the dipole tilt. The figure also shows the satellite positions (red dots) for the 80 satellite scenario. For each satellite the field line that intersects the satellite position is also drawn. Because the dipole, and thus the plasma sheet, is tilted with respect to the GSE equatorial plane, not all of the satellites are located in the plasma sheet, but a number of them also occupy the tail lobes. By inspection of the satellite positions relative to the plasma boundaries, and the magnetic topology of the field lines that the satellites intercept, it is clear that all relevant regions for the substorm process are sampled. In particular, the satellites in the plasma sheet sample areas where depolarization occurs, the inflow region of magnetic reconnection around  $-25 R_E$ , the outflow regions of reconnection both earthward and tailward of the X-line, as well as the adjacent regions in the tail flanks and in the tail lobes. Furthermore, there are numerous close conjunctions where 2-5 satellites cluster within 2-3  $R_E$  distance from each other. Such conjunctions provide excellent opportunities to measure boundary layer thicknesses, and the propagation speed and directions of disturbances. In many cases, these clusters should also provide the opportunity to measure the current vector directly from  $\nabla \times \mathbf{B}$ , as it has been proposed for the four satellite Cluster mission [Khurana et al., 1996; Kepko et al., 1996; Khurana et al., 1998]. Using the global MHD model to assess the measurement capabilities with these clusters is not quite possible yet with the current global MHD models because of limited model resolution. However, an assessment of the capability to recon-

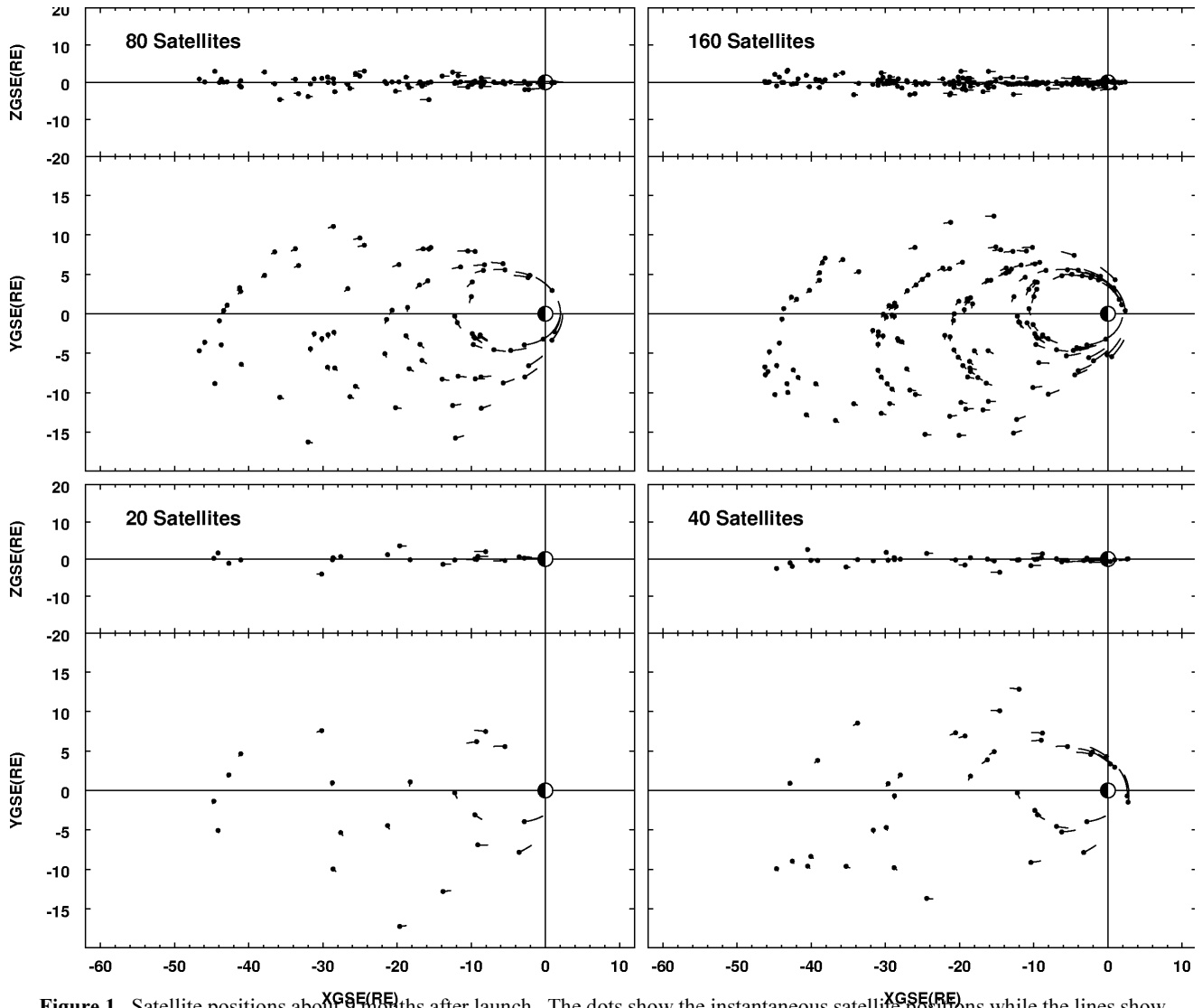


**Figure 1.** Satellite positions about 9 months after launch. The dots show the instantaneous satellite positions while the lines show 1 hour of orbit.

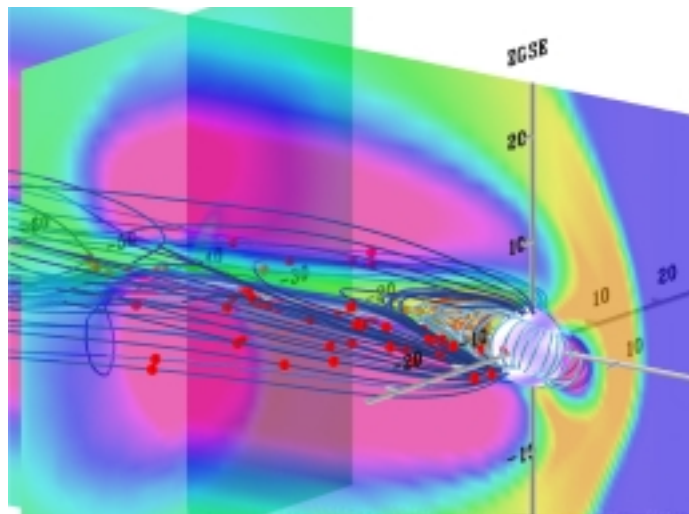


**Figure 2.** Rendering of the magnetosphere just after a substorm onset. The colored planes (at  $X_{GSE} = -40 R_E$  and  $Y_{GSE} = 0 R_E$ ) show color coded the plasma pressure. The sphere at the coordinate center shows the inner boundary of the simulation at  $3.5 R_E$ . The set of light blue field lines originates from  $66^\circ$  magnetic latitude and indicates the dipole tilt. The red dots show the satellite positions for the 80 satellite scenario. For each satellite the field line that intersects the satellite position is also drawn.

struct the global magnetospheric configuration and temporal evolution from multi-point measurements can be done.

#### 4. The Global Magnetospheric Configuration and Dynamics from Multipoint Measurements

Figures 3-6 show time series of several MHD variables around the substorm event for the four different configurations with 20, 40, 80 and 160 satellites, respectively. In order to examine the propagation of substorm features as a function of distance from Earth only satellites with  $X_{GSE} \leq -7 R_E$  and  $|Y_{GSE}| \leq 5 R_E$  are shown. This selection reduces the available satellites to 8, 12, 32, and 62, respectively, thus only about

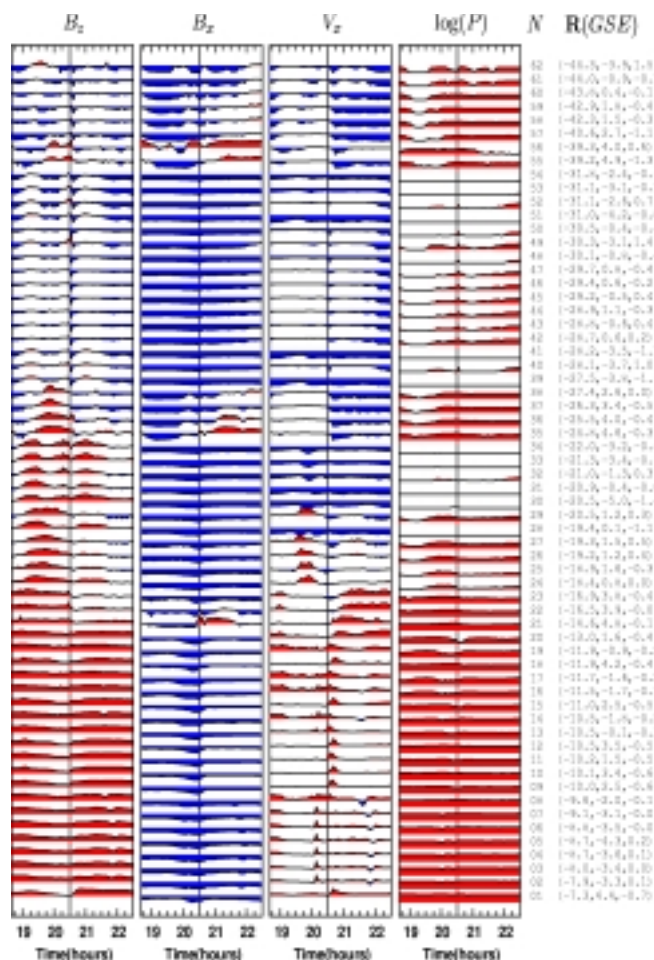


**Figure 3.** Time traces for the 160 satellite scenario. See text for details.

30 to 40 % of the available satellites are used. The time traces are further ordered by the satellite distance from Earth, with the most earthward satellites plotted at the bottom of the figures, and the most tailward at the top. The panels show, from left to right, the  $B_z$  component of the magnetic field, the  $B_x$  component of the magnetic field, the  $V_x$  component of the plasma velocity, and the logarithm of the plasma pressure  $\log(P)$ . The values of  $P$  range from approximately 0.01 to 1 nano Pascals. The values of  $V_x$ ,  $B_x$ , and  $B_z$  are scaled to their maximum absolute values for each of the time series, while preserving their sign, in order to make the important features, which are all temporal changes in the respective quantities, better visible. The black line at 20:10 UT marks the onset of a substorm. This onset is not only determined by

the tail signatures, but also by ionospheric signatures, such as auroral brightening and a sudden drop of the AL index (not shown here).

Clearly, the 160 satellite configuration (Figure 3) provides the most information and will thus be discussed first. Most of the substorm features can be identified in the  $B_z$  time traces. All satellites closer to Earth than about  $14 R_E$  observe a  $B_z$  increase at substorm onset, indicating the depolarization of the near Earthfield. From the resolution of the simulation it is not possible to determine if the depolarization is propagating earthward or tailward. However, by using real spacecraft data with about one second time resolution it should be possible to determine the propagation direction without any ambiguities. Beyond  $18 R_E$  the  $B_z$  signature is distinctively different. The  $B_z$  values first become negative for a brief period, and then depolarize to positive values. This is the signature of a small plasmoid or flux rope that develops because of the formation of a new near Earth X-line at around  $-17 R_E$ , and the subsequent retreat of this X-line. Note, that the two satellites located further at dawn (36 and 37) observe this feature about 15 minutes later, showing that the X-line is initially of very limited extent, but spreads later in the dawn-dusk direction. Another transition occurs beyond  $-26 R_E$ . Here,  $B_z$  is already negative before the onset. However, just before the onset  $B_z$  approaches zero and becomes positive at most satellites, thus the “distant” X-line, which was located around  $-26 R_E$  before onset moves tailward during the growth phase. At onset,  $B_z$  evolves to become strongly negative due to formation of the near Earth X-line and the plasmoid/flux rope ejection.

The  $B_x$  values are negative at most satellites, i.e., the satellites are located south of the neutral sheet. At all distances out to about  $-32 R_E$  the substorm growth phase is evident by an increase of the  $|B_x|$  values, except for some satellites that are apparently very close to the neutral sheet (21,22,35-38). At distances of  $-35 R_E$  and beyond the variations in  $B_x$  appear to be mainly due to the motion of the tail. At substorm onset, the  $|B_x|$  values start to decrease at most satellites, indicating the removal of tail flux due to the departure of the plasmoid/flux rope. Due to the limited resolution of the simulation it is difficult to determine the loading-unloading inflection point for each of the time traces. By using high resolution magnetometer data from MSM spacecraft, however, this should be possible. Tracing the inflection point through the satellite positions would then give an accurate determination of the plasmoid/flux rope motion.

Clear transitions are also present in the  $V_x$  velocity component with increasing distance from Earth. Within  $16 R_E$  from Earth the flows are Earthward-directed and bursty. The small flow bursts, reminiscent of Bursty Bulk Flows (BBFs) [Baumjohann *et al.*, 1990; Angelopoulos *et al.*, 1992, 1994] seen at satellites 2-7 to occur at around 20:10 UT correspond to a pseudo-breakup-like feature in the ionosphere (small dip in AL, not shown here). As with the depolarization front it is presently not possible to resolve these features well enough to determine their propagation direction, but with 5-10 second resolution flow measurements one should certainly be able to do so. Beyond  $X_{GSE} = -16 R_E$  the flows are almost entirely tailward. Some satellites observe a tailward flow that appears not to change very much at substorm onset. These satellites tend to be located further to the flanks. At the other satellites the tailward flow strongly increases at onset, coincident with the formation and departure of the plasmoid/flux rope.

The time traces of the plasma pressure also show a number of signatures that are often observed at substorms. Closer to Earth than about  $16 R_E$ , the pressure increases at substorm onset, coincident with the field depolarization. This is at some satellites preceded by a pressure decrease, but never by a plasma sheet drop out. This may be due to the fact that the satellites are all very close to the neutral sheet, and in part also due to lack of resolution in the model. Further tailward,

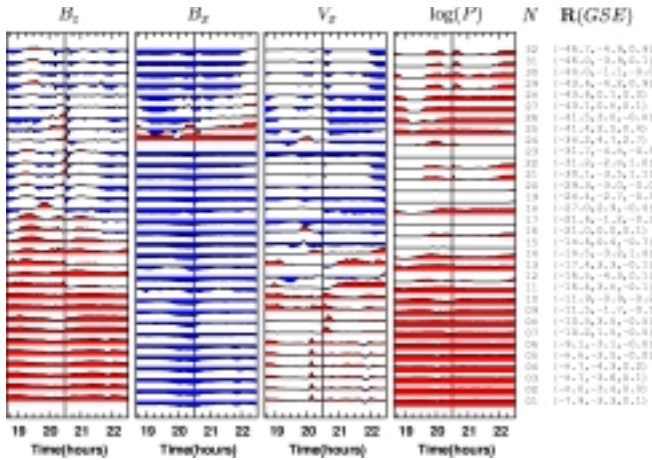


**Figure 4.** Time traces for the 80 satellite scenario. See text for details.

several satellites observe a plasma sheet dropout, however, only well after substorm onset. Apparently, the post plasmoid plasma sheet becomes very thin to allow these satellites to enter the lobe.

How much information would be lost if fewer than 160 satellites were employed? Figure 4 shows the time traces for 80 satellites. Every important substorm signature that is present in the 160 satellite analysis is still present in the 80 satellite scenario. However, some of the important propagating features, such as the depolarization front and the bursty bulk flows may be much more difficult to analyze. One should keep in mind that these features propagate both radially and azimuthally. Thus, if only very few ( $\leq 4$ ) such observations are available, ambiguities remain as to whether a structure moves radially inward or outward. In Figure 4 there are only 2 clear BBF signatures compared to 9 clear BBF signatures in the 160 satellite case. Thus for this event the determination of the BBF propagation may not be possible, and one may have to look for a different event that produces a clearer signature. For the depolarization front, however, there appear to be enough observations to determine its direction unambiguously in this case.

The information content drastically decreases in the cases with 40 and 20 satellites (Figures 5 and 6). Although the 40 satellite case still shows the transitions in  $B_z$  and  $V_x$  associated with the formation of the new X-line, an exact determination of the initial X-line location is more difficult, but would still yield the right answer. However, there are only 3 satellites that observe depolarization, and none that observe bursty flows. Thus, addressing the critical questions of disturbance propagation would still require a fortuitous satellite constellation. Finally, with 20 satellites the tail coverage becomes so poor that concise statements about the tail evolution become very difficult to make. The near Earth X-line location can at best be constrained to lie somewhere between  $18 R_E$  and  $28 R_E$ , and there is not enough information to identify either the propagation of the depolarization front or the bursty flows.

## 5. Summary and Discussion

We have used global simulations of Earth's magnetosphere to assess the expected scientific return from a multi satellite mission in the magnetosphere. We devise 4 different scenarios with 20, 40, 80, and 160 satellites, respectively. During the season when the satellite orbits cover the magnetotail, we investigate what the satellites would see in the course of a typical substorm event. Although it is by no means clear or proven that the substorm scenario produced by the global simu-

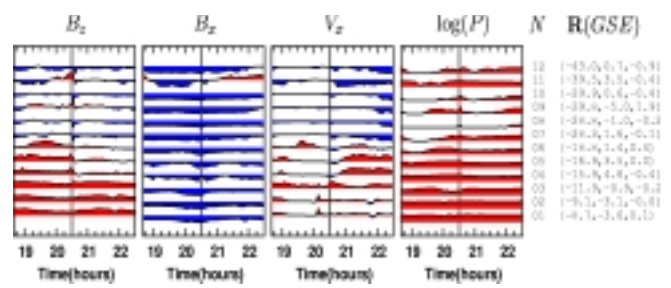


**Figure 5.** Time traces for the 40 satellite scenario. See text for details.

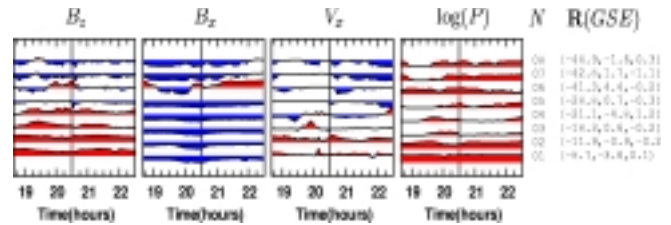


**Figure 6.** Time traces for the 20 satellite scenario. See text for details.

lation is correct in every respect (more likely not so), the simulated spacecraft scenario clearly shows which information can be extracted from multi spacecraft missions and how the information content depends on the number of satellites that are employed.

In the case of 160 satellites virtually all of the typically observed substorm signatures are seen by at least one satellite. Several key features, like the depolarization of the near Earth field and bursty bulk flows are seen at multiple ( $\geq 5$ ) satellites, which would allow an unambiguous determination of the propagation direction of these features. Although none of these “substorm observations” are anything new, and each of these signatures has been observed during typical substorms before, new information is to be gained from the fact that these observations are made simultaneously. This allows to put the different signatures in relation to each other *without spatial or temporal ambiguity*, and the time sequence of events in the course of a substorm can be established for the first time, not only for one or a few substorms, but for many. In this manner, phenomenological models, which at this point should be better called hypotheses, can be put to the test. Most likely, none of the current models would be fully consistent with the MSM observations, however, a more detailed and universally accepted model is likely to emerge.

Although a 160 satellite mission clearly appears to be capable to address the substorm problem in sufficient detail, it may still be beyond technical and budgetary means. A 80 satellite mission would still provide substantial tail coverage and the ability to observe all critical substorm signatures simultaneously for most events. However, with 80 satellites much statistical information will be lost, and it is much less likely that every substorm event will yield all the required information. In particular, the determination of propagation directions and speeds would suffer from poorer statistics, and the separation of radial from azimuthal propagation would be more difficult. Thus, with 80 satellites event selection becomes an issue, and it may be quite possible that different events may give apparently conflicting information on the time sequence that may be difficult to reconcile with one model.

A severe decrease of information content occurs when only 40 or 20 satellites are employed. In these cases it becomes virtually impossible to observe all substorm signatures simultaneously as required for

the elimination of substorm models/hypotheses. The studies that could be done with such missions can be expected to be similar to contemporary analyses, like event studies with limited scope, or statistical analysis, however with much larger data bases.

Of course, the analysis presented here is far from complete. Although we have tried to optimize the orbits with respect to the information that can be gained for substorms, it is conceivable that better orbit configurations can be devised. Also, we have only analyzed one substorm event which, although it appears to be a typical one, may not be a good representative for substorms in general. A more thorough study should include many more substorm events in order to investigate the limits of multi-satellite missions. A new problem that arises with multi-satellite missions is the presentation and analysis of the data, which has hitherto not received much attention. In this paper we presented the data as time series, which is a technique that is borrowed from data analysis of one or a few satellites, but may be inadequate and impractical for missions involving tens or hundreds of satellites. Much more sophisticated techniques to represent and analyze the data (for example "objective analysis") exist in neighboring disciplines like meteorology and oceanography [see eg. *Thiebaux and Pedder*, 1987]. By using these techniques, possibly in conjunction with data assimilation (see below), most likely more information can be readily extracted from multi-satellite data sets.

It should also be noted that the value of multi-satellite missions goes far beyond the study of substorms. In the course of a year the orbits sweep through several other important magnetospheric regions, such as the boundary layers, the magnetopause, the magnetosheath, the bow shock, and the solar wind just upstream of the bow shock. In each of those regions a multi-satellite mission provides far greater observing capabilities than any mission before. In particular, a multi-satellite mission would allow for measurements that are otherwise impossible, such as direct current density measurements [*Khurana et al.*, 1996; *Kepko et al.*, 1996; *Khurana et al.*, 1998], or measurements of the  $\omega - \mathbf{k}$  space of wave fields [*Neubauer and Glassmeier*, 1990].

In spite of the large satellite numbers, substantial regions of the magnetosphere would still not be covered by a multi-satellite mission. Thus global modeling of the magnetosphere would still be required to fill the observational gaps in order to get a complete picture of the magnetospheric configuration and dynamics. However, a multi-satellite mission would propel the field into a new era by providing for the first time sufficient data to use as input for data assimilation techniques in global magnetospheric models. These techniques are currently used with great success in atmospheric and ocean models [e.g., *Ghil and Malanotte-Rizzoli*, 1991; *Talagrand*, 1997; *Daley*, 1997]. The use of data assimilation in magnetospheric models would substantially improve their accuracy and provide the basis not only for improved phenomenological constructs, but for the understanding of the underlying physical processes as well.

**Acknowledgments.** This research was sponsored by NASA grant NAG5-4684 and NSF grant ATM 97-13449 at UCLA. The model computations were carried out on the IBM-SP2 at the San Diego Supercomputer Center. IGPP publication 5223.

## References

- Angelopoulos, V., et al., Statistical characteristics of bursty bulk flow events, *J. Geophys. Res.*, **99**, 21257, 1994.
- Angelopoulos, V., W. Baumjohann, C. F. Kennel, F. V. Coroniti, M. G. Kivelson, R. Pellat, R. J. Walker, H. Lühr, and G. Paschmann, Bursty bulk flows in the inner plasma sheet, *J. Geophys. Res.*, **97**, 4027, 1992.
- Baumjohann, W., G. Paschmann, and H. Lühr, Characteristics of high-speed ion flows in the plasma sheet, *J. Geophys. Res.*, **95**, 3801, 1990.
- Berchem, J., J. Raeder, M. Ashour-Abdalla, L. A. Frank, W. R. Paterson, K. L. Ackerson, S. Kokubun, Y. Yamamoto, and R. P. Lepping, The distant tail at 200  $R_E$ : Comparison between Geotail observations and the results from a global magnetohydrodynamic simulation, *J. Geophys. Res.*, **103**, 9121, 1998.
- Boden, D.G., Introduction to Astrophysics, in *Space mission Analysis and Design*, edited by J.R. Wertz and W.J. Larson, Kluwer Academic, Norwell, Mass., 1991.
- Daley, R., Atmospheric data assimilation, in *Data Assimilation in Meteorology and Oceanography: Theory and Practice*, edited by M. Ghil, and K. Ide, p. 209, Meteorological Society of Japan and Universal Academy Press, 1997.
- Frank, L. A. et al., Observations of plasmas and magnetic fields in Earth's distant magnetotail: Comparison with a global MHD model, *J. Geophys. Res.*, **100**, 19177, 1995.
- Ghil, M., and P. Malanotte-rizzoli, Data assimilation in meteorology and oceanography, *Advances in Geophysics*, **33**, 141, 1991.
- Kepko, L., K. K. Khurana, M. G. Kivelson, R. C. Elphic, and C. T. Russell, Accurate determination of magnetic field gradients from four point vector measurements - Part I: Use of natural constraints on vector data obtained from a single spinning spacecraft, *IEEE Transactions on Magnetics*, **32**, 377, 1996.
- Khurana, K. K., L. Kepko, M. G. Kivelson, and R. C. Elphic, Accurate determination of magnetic field gradients from four point vector measurements - Part II: Use of natural constraints on vector data obtained from four spinning spacecraft, *IEEE Transactions on Magnetics*, **32**, 5193, 1996.
- Khurana, K. K., L. Kepko, and M. G. Kivelson, Measuring magnetic field gradients from four point vector measurements in space, **103**, 311, 1998.
- Neubauer, F. M., and K. H. Glassmeier, Use of an array of satellites as a wave telescope, *J. Geophys. Res.*, **95**, 19115, 1990.
- Raeder, J., Global MHD simulations of the dynamics of the magnetosphere: Weak and strong solar wind forcing, in Proceedings of the Second International Conference on Substorms, edited by J. R. Kan, J. D. Craven, and S.-I. Akasofu, p. 561, Geophysical Institute, Univ. of Alaska Fairbanks, 1995.
- Raeder, J., et al., Boundary layer formation in the magnetotail: Geotail observations and comparisons with a global MHD model, *Geophys. Res. Lett.*, **24**, 951, 1997.
- Raeder, J., J. Berchem, and M. Ashour-Abdalla, The importance of small scale processes in global MHD simulations: Some numerical experiments, in *The Physics of Space Plasmas*, edited by T. Chang, and J. R. Jasperse, vol. 14, p. 403, Cambridge, Mass., MIT Cent. for Theoret. Geo/Cosmo Plasma Phys., 1996.
- Raeder, J., J. Berchem, and M. Ashour-Abdalla, The geospace environment modeling grand challenge: Results from a global geospace circulation model, *J. Geophys. Res.*, **103**, 14787, 1998.
- Talagrand, O., Assimilation of observations, an introduction, in *Data Assimilation in Meteorology and Oceanography: Theory and Practice*, edited by M. Ghil and K. Ide, p. 81, Meteorological Society of Japan and Universal Academy Press, 1997.
- Thiebaux, H. J., and M. A. Pedder, *Spatial Objective Analysis*, Academic Press, London, 1987.

Joachim Raeder, Institute of Geophysics and Planetary Physics, University of California at Los Angeles, 405 Hilgard Avenue, Los Angeles, CA 90095-1567. (email: jraeder@igpp.ucla.edu)